OBSERVER-BASED ADAPTIVE SECURE CONTROL WITH NONLINEAR GAIN RECURSIVE SLIDING-MODE FOR NETWORKED NON-AFFINE NONLINEAR SYSTEMS UNDER DOS ATTACKS

Yang Yang, Qing Meng, Dong Yue, Tengfei Zhang, Bo Zhao and Xiaolei Hou

We address the secure control issue of networked non-affine nonlinear systems under denial of service (DoS) attacks. As for the situation that the system information cannot be measured in specific period due to the malicious DoS attacks, we design a neural networks (NNs) state observer with switching gain to estimate internal states in real time. Considering the error and dynamic performance of each subsystem, we introduce the recursive sliding mode dynamic surface method and a nonlinear gain function into the secure control strategy. The relationship between the frequency (duration) of DoS attacks and the stability of the system is established by the average dwell time (ADT) method. It is proven that the system can withstand the influence of DoS attacks and track the desired trajectory while preserving the boundedness of all closed-loop signals. Finally, simulation results are provided to verify the effectiveness of the proposed secure control strategy.

Keywords: networked control system, secure control, adaptive control, dynamic surface control

Classification: 93D21, 93A15, 93D15

1. INTRODUCTION

Cyber-physical systems (CPSs) have been extensively studied over the past decade. A CPS is a large-scale interconnected complex system consisting of computing, communication and control components [13, 22] and finds its fitting application in areas, such as industrial process control [24], wireless sensor networks [10, 15, 35], multi-agent systems [3, 6, 7, 11, 52], intelligent buildings and power grids [14, 40].

Fruitful results have been available to deal with various control problems for pure-feedback nonlinear systems, one of the typical CPSs. For example, for a single-input-single-output (SISO) system with known model, Boubakir [2] presented a linear adaptive control algorithm. For uncertain systems, Chen et al. [4] employed neural networks (NNs) to deal with uncertainties and constructed an observer to estimate unknown system states. In [2, 4], it was required of repeated derivations of virtual control law in

the backstepping method, which might result in complexity computation along with the increasement of the relative order of the system. To overcome the problem of 'computational explosion', Swaroop et al. [33] proposed a dynamic surface control (DSC) technology. By introducing a first-order low-pass filter at each design step, the repeated derivation of the virtual control law was avoided. This technology was further developed combining with either NNs or fuzzy logic systems (FLSs) for pure-feedback nonlinear systems [8, 18, 29, 43, 49, 51]. However, there exist two drawbacks in the DSC results [18, 49]. One is the perturbation sensitivity issue within the controller parameters, and the other is the contradiction between the control accuracy and dynamic performance. For this purpose, enormous efforts have been attempted to improve the conventional DSC technology. On one hand, the error relationship among all subsystems, instead of local error reverse sequence, was considered. On the basis of this relationship, the recursive sliding-mode [37, 39] was employed to enhance the non-sensitiveness to controller's parameters. Liu et al. [19] and Shen et al. [27], combining recursive sliding-mode with NN adaptive DSC method, realized state feedback and output feedback control, respectively. On the other hand, a nonlinear gain function [16] from engineering experience was introduced into nonlinear systems to coordinate the contradiction between control accuracy and dynamic performance. The work in [19] was further developed in [20] via a nonlinear gain function to replace the linear gain in the traditional DSC method. The imptoved technology was applied to solve the tracking control problem for uncertain multiple-input-multiple-output (MIMO) systems in [28].

Due to the fact that the connections, between nonlinear systems and sensors in physical and network space, are vulnerable, the secure control problem has been widely concerned. One of the typical malicious cyber-attacks is the denial of service (DoS) [26]. The aim of DoS attacks is to jam communication information in the transmission channel. Without accessible information, most control schemes are not able to be applied directly, which may lead to degraded performance or even instability. A large number of research results [1, 16, 19, 20, 25, 27, 28, 30–32, 37, 48] mainly focus on how to defence DoS attacks. Compared with the most existing single-channel method, Lu et al. [21] studied the security control problem of CPS systems with multiple transmission channels under DoS attack. With the switched system technology [44, 45, 47], sufficient conditions in terms of DoS attacks parameters were obtained for guaranteeing the system stability. Taking limited energy resources of real-world jammers into consideration, Hu et al. developed an event-based sampling scheme in [12] to tackle period DoS jamming attacks. By introducing an event triggered mechanism, a switching model related to state error was constructed and a segmented Lyapunov function was selected to prove the global stability of the system. It was shown that both the security control performance and the economical communication resource consumption can be evaluated in a unified framework.

Inspired by the discussions above, for a non-affine nonlinear system in the presence of intermittent DoS attacks, we develop an observer-based adaptive dynamic surface secure control strategy with nonlinear gain and recursive sliding-mode. In this paper, an NN observer is designed based on discontinuous system output signal. In the design of the secure strategy, we take the errors among subsystems into account and design recursive sliding-mode, which release the sensitiveness to perturbation of control parameters. Fur-

thermore, we introduce a simple nonlinear gain function, instead of a linear gain, into the traditional DSC method, aiming to improve the dynamic performance. Combining the property of DoS attack with the ADT method, the overall uniform boundedness of the system is proved by Lyapunov function. The main contributions of this paper are as follows.

(1) An adaptive output feedback secure control strategy is proposed for non-affine nonlinear systems in the presence of DoS attacks. Unlike the system models in [1, 19], the plant in this paper is more general, and the results in [1, 19] can be regarded as one of special cases of this study. Moreover, compared with [18, 20, 28, 49], an adaptive secure control strategy with switching gain observer is designed of nonlinear systems suffered from DoS attacks. The relationship between the attack parameters and control performance is analyzed.

(2) Recursive sliding-mode and nonlinear gain are introduced into the secure control in this paper. Compared with conventional DSC method in [1, 49], the strategy in this paper is constructed by the errors among each subsystems and releases the sensitiveness to perturbation of control parameters.

The rest of this paper is organized as follows. In Section 2, we present the problem formulation and preliminaries. In Section 3 and Section 4, we propose a secure control strategy and analyze the system stability, respectively. Simulation results are presented in Section 5, and then, in Section 6, we draw some conclusions.

2. PROBLEM FORMULATION AND PRELIMINARIES
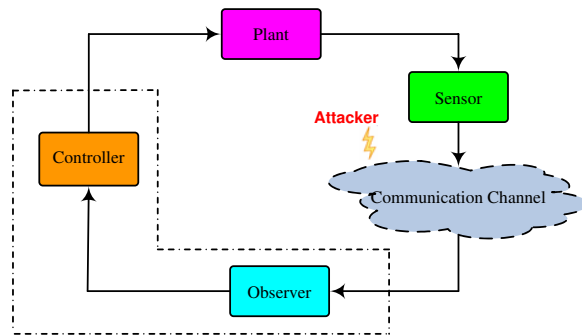
2.1. Problem description

Fig. 1: The diagram of the networked system in the presence of DoS attacks

The diagram of the networked system in the presence of DoS attacks is shown in Figure 1. The signal transmission between the sensor and the observer is implemented through a wireless transmission channel which might be blocked by malicious DoS jam-

mers. The dynamics of the system are

$$\begin{cases} \dot{x}_i = f_i\,(\overline{x}_i, x_{i+1}), \\ \dot{x}_n = f_n\,(\overline{x}_n, u), \\ y = x_1, \end{cases} \tag{1}$$

where $i = 1, \ldots, n$, $\overline{x}_i = [x_1, x_2, \ldots, x_i]^T \in \mathbb{R}^i$ is a state vector consisting of unavailable state variable x_i, u and y are the control signal and the output information of the system, respectively, $f_i(\cdot)$ is an unknown nonlinear function with its first-order being continuous and derivable.

Let

$$F_i\,(\overline{x}_i, x_{i+1}) = f_i\,(\overline{x}_i, x_{i+1}) - x_{i+1},$$

$$F_n\,(\overline{x}_n, u) = f_n\,(\overline{x}_n, u) - u.$$

The system (1) is equivalent to the following nonlinear system

$$\begin{cases} \dot{x}_i = F_i\,(\overline{x}_i, x_{i+1}) + x_{i+1}, \\ \dot{x}_n = F_n\,(\overline{x}_n, u) + u, \\ y = x_1. \end{cases} \tag{2}$$

Throughout this paper, some common assumptions are necessary.

Assumption 1. The reference signal y_d and its derivatives $\dot{y}_d$ and $\ddot{y}_d$ exist, and the signal y_d satisfies $y_d \in \Omega_1 = \left\{ (y_d, \dot{y}_d, \ddot{y}_d) \,|\, y_d^2 + \dot{y}_d^2 + \ddot{y}_d^2 \leq C_0 \right\}$, where $C_0 > 0$.

Assumption 2. (Li, Tong, and Li [18]) For the continuous function $F_i(\cdot)$, $i = 1, \ldots, n$, it is Lipschitz. That is, there exists a positive constant m_i such that, for any $X_1 \in \mathbb{R}^{i+1}$ and $X_2 \in \mathbb{R}^{i+1}$, the inequality $\|F_i\,(X_1) - F_i\,(X_2)\| \leq m_i \,\|X_1 - X_2\|$ holds.

We introduce the Butterworth low-pass filter $H_{\mathrm{L}}(s)$ to avoid the algebraic loop problem [53], and define the filtered signals $\hat{x}_{i+1,f} = H_{\mathrm{L}}(s)\hat{x}_{i+1}$ and $u_f = H_{\mathrm{L}}(s)u$, where $\hat{x}_{i+1}$ is the estimation of system state obtained by the observer and the more details will be given in Section 3. Rewrite system (2) as

$$\begin{cases} \dot{x}_i = F_i\,(\underline{\hat{x}}_i, \hat{x}_{i+1,f}) + \Delta F_i + x_{i+1}, \\ \dot{x}_n = F_n\,(\underline{\hat{x}}_n, u_f) + \Delta F_n + u, \\ y = x_1, \end{cases} \tag{3}$$

where $\underline{\hat{x}}_i = \left[\hat{x}_1, \hat{x}_2, \ldots, \hat{x}_i\right]^T$. And, $\Delta F_i = F_i\,(\overline{x}_i, x_{i+1}) - F_i\,(\underline{\hat{x}}_i, \hat{x}_{i+1,f})$, $\Delta F_n = F_n\,(\overline{x}_n, u) - F_n\,(\underline{\hat{x}}_n, u_f)$.

Assumption 3. (Li, Tong, and Li [18]) There exist positive constants $\tau_{j,0}$, $j = 1, \ldots, n$, $n+1$, such that $|\hat{x}_i - \hat{x}_{i,f}| \leq \tau_{i,0}$, $i = 1, \ldots, n$, $|u - u_f| \leq \tau_{n+1,0}$.

Remark 2.1. For a pure-feedback nonlinear system (1), the virtual control law is often designed as $\alpha_2 = -g_1\chi_1 - \hat{f}_1\,(\overline{x}_1, x_2) + \dot{y}_d$, $\alpha_{i+1} = -g_i\chi_i - \hat{f}_i\,(\overline{x}_i, x_{i+1}) + \dot{\alpha}_i - \chi_{i-1}$, $i = 2, \ldots, n-1$, where $\chi_1 = x_1 - y_d$, $\chi_j = x_j - \alpha_j$, $j = 2, \ldots, n$, g_i is a positive constant, $\hat{f}_i\,(\overline{x}_i, x_{i+1})$ is the estimation of $f_i\,(\overline{x}_i, x_{i+1})$, and y_d is the reference trajectory. From

the aforementioned expressions of virtual control laws in this remark, the signal x_{i+1} is used in α_{i+1}, and it mainly manifests that $\hat{f}_i(\overline{x}_i, x_{i+1})$ depends on the signal x_{i+1} in the NNs and x_{i+1} appears on both sides of α_{i+1}. This will lead to so-called 'algebraic loop problem' and the virtual control law cannot be implemented directly in practice. In this paper, the algebraic loop problem is circumvented by introducing the Butterworth low-pass filter. More details about this filter and the corresponding filter parameters can be referenced in [53].

2.2. Nonlinear gain function

In this paper, we introduce a continuous and differentiable nonlinear gain function $f_z(x)$ of the following form

$$f_z(x) = \lambda |x|^{\frac{1}{2}} \operatorname{sgn}(x), \tag{4}$$

where λ is a positive constant. The function holds the following properties for the convenience of stability analysis.

Property 1. The derivative of the nonlinear gain function is

$$\frac{df_z(x)}{dx} = \begin{cases} 1, & \text{if } x = 0, \\ \dfrac{\lambda}{2}|x|^{-\frac{1}{2}}, & \text{if } x \neq 0. \end{cases} \tag{5}$$

Property 2. Define a differentiable function

$$l(x) = \frac{1}{2}\left[\frac{df_z(x)}{dx}x + f_z(x)\right] \tag{6}$$

and, for any $x \in \mathbb{R}$, it satisfies

$$x \cdot l(x) = \frac{1}{2}\left[\frac{df_z(x)}{dx}x^2 + x \cdot f_z(x)\right] \geq \frac{1}{2}x \cdot f_z(x). \tag{7}$$

Property 3. Define a piecewise function

$$N(x) = \begin{cases} 1, & \text{if } x = 0, \\ \dfrac{l(x)}{x}, & \text{if } x \neq 0, \end{cases} \tag{8}$$

and, for any $x \in \mathbb{R}$, the inequality $N(x) > 0$ holds.

2.3. Intermittent DoS attack model

The DoS attack is one of common threats in CPSs. In this paper, we assume that only the communication channel between the sensor and observer is interrupted. That is, the control strategy might not receive signal from the sensor devices through the communication channel. Meanwhile, we only consider the situation that an intelligent
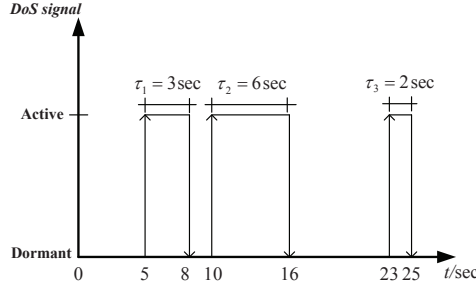
Fig. 2: Example of DoS signal

adversary performs intermittent DoS attacks in a purely continuous-time setting, and it means that an attacker can only launch DoS attack intermittently.

From the method in [25], we denote $E_k := [t_k, t_k + \tau_k)$ represents time interval of the kth DoS attack, where t_k, $k \in N$ and $t_0 \geq 0$, is starting instant of the kth attack, and $\tau_k \in \mathbb{R}^+$ is attack duration. During the period $[t_k, t_k + \tau_k)$, network communication is aborted. And on the each interval $[\tau, t]$, denote $\Phi(\tau, t) := \bigcup_{k \in N} E_k \bigcap [\tau, t]$ and $\Psi(\tau, t) := \frac{[\tau, t]}{\Phi(\tau, t)}$ represent the sets of time instants where communication is aborted and allowed, respectively. Further, $|\Phi(\tau, t)|$ and $|\Psi(\tau, t)|$ represent the total lengths of DoS attack being active or dormant in $[\tau, t]$, respectively. Therefore, the actual output of the system can be described as

$$\breve{y}(t) = \begin{cases} 0, & t \in \Phi(0, +\infty), \\ y(t), & t \in \Psi(0, +\infty). \end{cases} \tag{9}$$

Let $n(\tau, t)$ denote the number of DoS *dormant/active* transitions in $[\tau, t]$. To describe the intermittent nature of DoS attack, some assumptions of the DoS character are given.

Assumption 4. (Persis and Tesi [25]) There exist constants $\kappa \geq 0$ and τ_D such that the inequality $n(\tau, t) \leq \kappa + \frac{t - \tau}{\tau_D}$ holds.

Assumption 5. (Persis and Tesi [25]) For any $\tau, t \geq 0$ and $\tau \leq t$, there exists a constant $\omega \geq 0$ and $\varrho > 1$ satisfying $|\Phi(\tau, t)| \leq \omega + \frac{t - \tau}{\varrho}$.

Remark 2.2. An example of DoS signal in this paper is shown in Figure 2. In Figure 2, *dormant/active* transitions are represented as $\uparrow$, while *active/dormant* transitions are represented as $\downarrow$. *Dormant/active* transitions occur at 5s, 10s, and 23s and the corresponding DoS intervals have duration 3s, 6s, and 2s, respectively. This yields for instance: $n(0, 1) = 0$, $n(3, 13) = 2$, and $n(7, 25) = 3$, while $\Phi(0, 1) = \phi$, $\Phi(3, 13) = [5, 8) \cup [10, 13)$, and $\Phi(7, 25) = [7, 8) \cup [10, 16) \cup [23, 25)$.

Remark 2.3. From Assumption 4, the constant τ_D is called the 'average dwell time' [46, 47] and represents a parameter whose inverse provides an upper bound on the average frequency of DoS *dormant/active* transitions in this paper. The idea is that there may exist some consecutive switchings separated by less than τ_D, but the average interval between consecutive switchings is no less than τ_D. In fact, Assumption 4 indicates that if we ignore the first switchings, the average time interval between consecutive switchings is at least τ_D.

Remark 2.4. Assumption 4 and Assumption 5 are necessary conditions to guarantee the controllability of the system under the DoS attack. On one hand, if the frequency of DoS attack is infinite and the duration is limited, the attacker can perform multiple attacks at short intervals within a certain time interval. If the time interval of attack activity is significantly longer than the time interval of attack dormancy, that is, the parameter ϱ is smaller than 1. Given that data is only sent at a certain instant in a certain interval, in the worst case, all data might not be sent. On the other hand, if the frequency of DoS attack is limited and the duration is unlimited, the DoS attack may never stop and all data will not be sent. Therefore, if the duration or frequency of a DoS attack is infinite, the system will be unstable. As seen from [25] and [9], Assumption 4 and Assumption 5 are reasonable and reflect the energy constraint on the DoS attack. It is assumed that the relationship between the length and time span is linear with the unity control gain. In fact, for a single DoS attack, from [25] and Assumption 5 with $\tau = t_k$ and $t = t_k + \tau_k$, it implies $\sup_{k \in N} \tau_k \leq \omega \varrho / (\varrho - 1)$. The duration of an attack τ_k is increased, and $|\Phi(\tau, t)|$ is extended. The impact from this situation will be discussed detailed in Remark 4.3.

2.4. RBF NNs

Neural networks are usually employed in the results on uncertain nonlinear system control to approximate unknown dynamics. The form of the approximation of an unknown continuous function $f_i(Z_i)$ is

$$f_i(Z_i) = \theta_i^{*T} S_i(Z_i) + \varepsilon_i(Z_i), \tag{10}$$

where $Z_i = \left[z_{i,1}, z_{i,2}, \ldots, z_{i,q} \right]^T \in \mathbb{R}^q$ is the input vector, $\theta_i^* = \left[\theta_{i,1}^*, \theta_{i,2}^*, \ldots, \theta_{i,p}^* \right]^T \in \mathbb{R}^p$ is the idea weight vector, $\varepsilon_i(Z_i)$ is the approximation error, $S_i(Z_i) = \left[s_{i,1}(Z_i), s_{i,2}(Z_i), \ldots, s_{i,p}(Z_i) \right]^T \in \mathbb{R}^p$ is the radial basis function, and the following Gaussian function $s_{i,j}(Z_i) = \exp \left[-\frac{(Z_i - b_j)^T (Z_i - b_j)}{\eta_i^2} \right]$ is chosen, where $j = 1, 2, \ldots, p$, $b_j = \left[b_{j,1}, b_{j,2}, \ldots, b_{j,q} \right]^T$ and η_i are the center and its width, respectively. The idea weight value θ_i^* is unavailable, and the estimation weight $\hat{\theta}_i$ is introduced with the definition of the estimation error $\widetilde{\theta}_i = \hat{\theta}_i - \theta_i^*$.

Assumption 6. The ideal weight of the neural networks θ_i^* is bounded, that is, there exists $\theta_M > 0$ such that $\|\theta_i^*\| \leq \theta_M$.

In this paper, we employ NNs for estimating the unknown nonlinear function $F_i(\underline{\hat{x}}_i, \hat{x}_{i+1,f})$ in

$$\hat{F}_i \left(\underline{\hat{x}}_i, \hat{x}_{i+1,f} | \hat{\theta}_i \right) = \hat{\theta}_i^T S_i \left(\hat{x}_i, \hat{x}_{i+1,f} \right). \tag{11}$$

We further define the minimum approximation error ε_i

$$\varepsilon_i = F_i \left(\underline{\hat{x}}_i, \hat{x}_{i+1,f} \right) - \hat{F}_i \left(\underline{\hat{x}}_i, \hat{x}_{i+1,f} | \theta_i^* \right) \tag{12}$$

and the approximation error δ_i

$$\delta_i = F_i \left(\underline{\hat{x}}_i, \hat{x}_{i+1,f} \right) - \hat{F}_i \left(\underline{\hat{x}}_i, \hat{x}_{i+1,f} | \hat{\theta}_i \right). \tag{13}$$

Assumption 7. The bounds of the neural networks minimum approximation error ε_i and approximation error δ_i are ε_{iM} and δ_{iM}, respectively.

Denote $\rho_i = \varepsilon_i - \delta_i$. According Assumption 7, there exists an unknown constant $\rho_i^* > 0$ such that $|\rho_i| \leq \rho_i^* = \varepsilon_{iM} + \delta_{iM}$.

Remark 2.5. RBF NNs have the ability of approximating continuous smooth functions. However, it is difficult to obtain either the idea weight value θ^* or the approximation error ε_i and δ_i bounds in practice. In this paper, several adaptive laws will be developed to estimate the idea weight value and these bounds in the following section, respectively.

The control objective of this paper is to design an adaptive output feedback secure control strategy for the non-affine pure-feedback system (1) in the presence of intermittent DoS attack in the sense that the strategy steers the output y to track the reference signal y_d while the tracking error $\epsilon = y - y_d$ converges to a small neighborhood around the origin.

3. SECURE CONTROL STRATEGY DESIGN

In this section, we will present the design process of adaptive secure control strategy, including NN state observer and control input signal. The stability analysis of the overall system will be given in the following section.

3.1. Neural network state observer

Recalling that the system state variables are unavailable, a state observer is thus designed to estimate these unknown states. Denote $\hat{x}_{n+1,f} = u_f$ and rewrite (3) in the state-space form

$$\begin{cases} \dot{x} = Ax + \sum_{i=1}^{n} B_i F_i \left(\hat{\underline{x}}_i, \hat{x}_{i+1,f} \right) + Bu + \Delta F, \\ y = x_1, \end{cases} \tag{14}$$

where $x = [x_1, x_2, \ldots, x_n]^T$, $A = \begin{bmatrix} 0 & 1 & 0 & \cdots & 0 \\ 0 & 0 & 1 & \cdots & 0 \\ \vdots & \vdots & \vdots & \ddots & \vdots \\ 0 & 0 & 0 & \cdots & 1 \\ 0 & 0 & 0 & \cdots & 0 \end{bmatrix} \in \mathbb{R}^{n \times n}$, $B = \begin{bmatrix} 0 \\ \vdots \\ 1 \end{bmatrix} \in \mathbb{R}^n$,

$B_i = [\underbrace{0, \ldots 0, 1}_{i}, 0, \ldots, 0]^T \in \mathbb{R}^n$, $\Delta F = \begin{bmatrix} \Delta F_1 \\ \vdots \\ \Delta F_n \end{bmatrix}$.

In this paper, we let $\vartheta = 1/0$ to judge whether the control module receives the output signal. According to (14), a state observer is designed as

$$\begin{cases} \dot{\hat{x}} = A\hat{x} + \sum_{i=1}^{n} B_i \hat{F}_i \left(\hat{\underline{x}}_i, \hat{x}_{i+1,f} | \hat{\theta}_i \right) + K^\vartheta \breve{e}_1 + Bu, \\ \hat{y} = \hat{x}_1, \end{cases} \tag{15}$$

where $K^\vartheta = \left[k_1^\vartheta, \cdots, k_n^\vartheta\right]^T$, $\breve{e}_1 = \breve{y} - \hat{x}_1$ and the adaptive law for $\hat{\theta}_i$ will be given later. When $t \in \Phi(0, +\infty)$, $\vartheta = 0$, $K^\vartheta = K^0$; otherwise, $\vartheta = 1$, $K^\vartheta = K^1$.

Define $e = x - \hat{x}$ as the estimation error of the observer, and we obtain the derivative of the observer error

$$\dot{e} = Ae + \Delta F + \delta - K^\vartheta \breve{e}_1, \tag{16}$$

where $e = \left[e_1, \cdots, e_n\right]^T$ and $\delta = \left[\delta_1, \cdots, \delta_n\right]^T$. Obviously, when $t \in \Phi(0, +\infty)$, $\breve{e}_1 = -\hat{x}_1$, and $\breve{e}_1 = e_1$ when $t \in \Psi(0, +\infty)$.

We take stability analysis for observer over the time intervals $t \in \Phi(0, +\infty)$ and $t \in \Psi(0, +\infty)$ by Lyapunov function $V_o = e^T P^\vartheta e$, respectively.

First, consider the time interval $t \in \Phi(0, +\infty)$, during this time period, $\breve{y} = 0$ and $\vartheta = 0$. The derivative of V_o is

$$\dot{V}_o = e^T \left(A^T P^0 + P^0 A\right) e + 2e^T P^0 \left(\Delta F + \delta + K^0 \hat{x}_1\right). \tag{17}$$

According to Young's inequality, Assumption 2–3, and Assumption 7, we have

$$2e^T P^0 \Delta F \leqslant \|e\|^2 \|P^0\|^2 + \left(|\Delta F_1|^2 + \cdots + |\Delta F_n|^2\right) \tag{18}$$
$$\leqslant r_0 \|e\|^2 + M_o,$$

$$2e^T P^0 \delta \leqslant \|e P^0\|^2 + \|\delta_M\|^2, \tag{19}$$

where $r_0 = \|P^0\|^2 + 2\sum_{i=1}^n m_i^2$, $M_o = 2\sum_{i=1}^n m_i^2 \tau_{i0}^2$.

Then, we can obtain

$$\dot{V}_o \leqslant e^T \left[A^T P^0 + P^0 A + 2P^0 P^0 + 2\sum_{i=1}^n m_i^2 + \hat{x}_1^2 P^0 K^0 K^{0T} P^0\right] e + \|\delta_M\|^2 + M_o. \tag{20}$$

Further, we consider the time interval $t \in \Psi(0, +\infty)$, during this time period, $\breve{y} = x_1, \vartheta = 1$. Similarly, it follows that

$$\dot{V}_o \leqslant e^T \left[\left(A - K^1 C_0\right)^T P^1 + P^1 \left(A - K^1 C_0\right) + 2P^0 P^0 + 2\sum_{i=1}^n m_i^2\right] e + \|\delta_M\|^2 + M_o, \tag{21}$$

where $C_0 = \left[1, 0, \cdots, 0\right] \in \mathbb{R}^{1 \times n}$.

Next, to obtain the whole system stability result in Section 4, the gain vector K^ϑ of the observer (15) should satisfies

$$A^T P^0 + P^0 A + 2P^0 P^0 + 2\sum_{i=1}^n m_i^2 + \hat{x}_1^2 P^0 K^0 K^{0T} P^0 < \upsilon P^0 \tag{22}$$

and

$$\left(A - K^1 C_0\right)^T P^1 + P^1 \left(A - K^1 C_0\right) + 2P^0 P^0 + 2\sum_{i=1}^n m_i^2 < -\nu P^1, \tag{23}$$

where υ and ν are positive constants.

In addition, the observer we designed should also be stable in the time interval $t \in \Phi(0, +\infty)$ with $u = 0$, so that K^0 satisfies

$$\left(A - K^0 C_0\right)^T P^0 + P^0 \left(A - K^0 C_0\right) + P^{0T} P^0 < 0. \tag{24}$$

Specially, the observer's gain K^ϑ satisfying (22)(23)(24) can be solved by LMI tool in [5, 41].

Remark 3.1. Adaptive output feedback control of nonlinear uncertain systems has been widely studied. In [8, 17, 18, 23, 36], several adaptive NN estimators have been constructed to estimate unknown states. However, these estimators are designed based on output measurements without any attacks, and they cannot be applied to our case since the sensor measurements are corrupted intermittently by malicious attackers. For comparison, in our proposed scheme, we treat the system attacked or not as two subsystems and obtain a marking signal $\vartheta = 1/0$ to judge whether the control module receives the output depending on the detection technology. According to the marking signal, the switching-type adaptive NN observer (15) is designed by the switched technique [44, 45, 47], and it estimates unknown states in stable and unstable uncertain nonlinear subsystems, respectively.

3.2. Adaptive secure control strategy

In this subsection, on the basis of the NN state observer (15), an adaptive secure control strategy is presented combining the recursive sliding-mode DSC with the nonlinear gain function. The whole design process is composed of n steps.

Step 1: Define the first sliding surface

$$\begin{cases} d_1 = \hat{x}_1 - y_d, \\ \chi_1 = d_1. \end{cases} \tag{25}$$

Deriving of χ_1, we obtain

$$\dot{\chi}_1 = \hat{\theta}_1^T S_1(\hat{\underline{x}}_1, \hat{x}_{2,f}) + k_1^\vartheta (\breve{y} - \hat{x}_1) + \hat{x}_2 - \dot{y}_d. \tag{26}$$

Accordingly, we design the virtual control law

$$\alpha_2 = -\hat{\theta}_1^T S_1 - k_1^\vartheta (\breve{y} - \hat{x}_1) - g_1 l_1(\chi_1) - \tanh\left(\frac{l_1(\chi_1)}{\xi}\right) \hat{\rho}_1 + \dot{y}_d \tag{27}$$

with adaptive laws

$$\dot{\hat{\theta}}_1 = \beta_1 [l_1(\chi_1) S_1 - \sigma_1 \hat{\theta}_1] \tag{28}$$

and

$$\dot{\hat{\rho}}_1 = \gamma_1 \left[\tanh\left(\frac{l_1(\chi_1)}{\xi}\right) l_1(\chi_1) - \Lambda(\hat{\rho}_1 - \rho_1^0) \right], \tag{29}$$

where $l_1(\chi_1)$ is defined in (6), $\hat{\rho}_1$ is the estimation of ρ_1, and $g_1, \xi, \beta_1, \sigma_1, \gamma_1, \Lambda$ and ρ_1^0 are positive parameters to be designed.

In order to avoid the computational complexity caused by repeated derivation of the virtual control law in the design process, we introduce a first-order low-pass filter with time constant T_2 of the following form

$$T_2 \dot{z}_2 + z_2 = \alpha_2, z_2(0) = \alpha_2(0), \tag{30}$$

where z_2 is the output signal of the filter.

Step $i(i \geq 2)$: Define the ith sliding surface

$$\begin{cases} d_i = \hat{x}_i - z_i, \\ \chi_i = c_{i-1}\chi_{i-1} + d_i, \end{cases} \tag{31}$$

and the derivative of χ_i is

$$\dot{\chi}_i = c_{i-1}\dot{\chi}_{i-1} + \hat{\theta}_i^T S_i + \hat{x}_{i+1} + k_i^{\vartheta}(\breve{y} - \hat{x}_1) - \dot{z}_i. \tag{32}$$

We design the virtual control law

$$\alpha_{i+1} = -c_{i-1}\dot{\chi}_{i-1} - \hat{\theta}_i^T S_i - k_i^{\vartheta}(\breve{y} - \hat{x}_1) - g_i l_i(\chi_i) - \tanh\left(\frac{l_i(\chi_i)}{\xi}\right)\hat{\rho}_i - \frac{l_{i-1}(\chi_{i-1})}{N_i(\chi_i)} + \dot{z}_i \tag{33}$$

with the adaptive laws

$$\dot{\hat{\theta}}_i = \beta_i[l_i(\chi_i)S_i - \sigma_i\hat{\theta}_i] \tag{34}$$

and

$$\dot{\hat{\rho}}_i = \gamma_i\left[\tanh\left(\frac{l_i(\chi_i)}{\xi}\right)l_i(\chi_i) - \Lambda(\hat{\rho}_i - \rho_i^0)\right], \tag{35}$$

where $N_i(\chi_i)$ is defined in (8) and $g_i, \xi, \beta_i, \sigma_i, \gamma_i, \Lambda, \rho_i^0, c_i$ are positive parameters to be designed.

Similarly, to avoid the 'computing explosion' caused by repeatedly differentiating the virtual control law, we introduce the first-order filter

$$T_{i+1}\dot{z}_{i+1} + z_{i+1} = \alpha_{i+1}, z_{i+1}(0) = \alpha_{i+1}(0) \tag{36}$$

with time constant T_{i+1}, where z_{i+1} is the output signal of the filter.

Step n: Define the nth sliding surface

$$\begin{cases} d_n = \hat{x}_n - z_n, \\ \chi_n = c_{n-1}\chi_{n-1} + d_n. \end{cases} \tag{37}$$

The derivation of χ_n is

$$\dot{\chi}_n = c_{n-1}\dot{\chi}_{n-1} + \hat{\theta}_n^T S_n + u + k_n^{\vartheta}(\breve{y} - \hat{x}_1) - \dot{z}_n. \tag{38}$$

Finally, we design the secure control strategy

$$u = -c_{n-1}\dot{\chi}_{n-1} - \hat{\theta}_n^T S_n - k_n^{\vartheta}(\breve{y} - \hat{x}_1) - g_n l_n(\chi_n) - \tanh\left(\frac{l_n(\chi_n)}{\xi}\right)\hat{\rho}_n$$
$$- c_n\chi_n - \frac{l_{n-1}(\chi_{n-1})}{N_n(\chi_n)} + \dot{z}_n \tag{39}$$

and the following adaptive laws

$$\dot{\hat{\theta}}_n = \beta_n\left[l_n(\chi_n)S_n - \sigma_n\hat{\theta}_n\right] \tag{40}$$

and

$$\dot{\hat{\rho}}_n = \gamma_n\left[\tanh\left(\frac{l_n(\chi_n)}{\xi}\right)l_n(\chi_n) - \Lambda(\hat{\rho}_n - \rho_n^0)\right], \tag{41}$$

where g_n, ξ, β_n, σ_n, γ_n, Λ, ρ_n^0 and c_n are positive parameters to be designed.

Remark 3.2. Backstepping method in [2, 4] has been widely applied for the class of nonlinear systems. However, the virtual control variables α_i were required to be repeatedly differentiated at each step and the computational complexity multiply along with the degree increasement of the system. In this paper, the DSC method [18, 49] is introduced to simplify the design process.

Remark 3.3. The conventional DSC method in [18, 49] is only based on local error reverse sequence. That is, the error $d_i < 0$ might lead to accelerate decreasement of d_{i-1}. In this situation, it would be beneficial for the system performance if $d_{i-1} > 0$, and the fact, $d_{i-1} < 0$, would bring negative impacts on the system performance. Note that the system error d_i cannot reflect the real-time tracking error $x_i - \alpha_i$ in conventional DSC because there exists an inevitable phase delay from the low-pass filter. Thus, it is sensitive for the controller to the perturbation of the parameters. In this paper, we define the recursive sliding surfaces (25), (31) and (37) for building error relationship among all subsystems to expand the range of control parameters.

4. STABILITY ANALYSIS

The main result of this paper is summarized in the following theorem.

Theorem 4.1. Consider the non-affine nonlinear system (1) in the presence of the DoS attack satisfying Assumption 1–Assumption 7. If there exist positive definite matrices P^0, P^1 and a positive constant π^* such that $P^0 < \mu P^1, P^1 < \mu P^0, \frac{\nu - \pi^*}{\nu + \upsilon} > \frac{1}{\varrho}, \pi^* > \frac{\ln\mu}{\tau_D}$ and choose $c_i > \nu, \frac{1}{T_i} - \frac{1}{2} - \frac{1}{4\zeta_i} > \nu, \sigma_i > \nu, \Lambda > \nu, g_i > \zeta_i$, the nonlinear gain recursive sliding-mode dynamic surface adaptive secure control strategy, including the NN state observer (15), the control signal input (39), and the adaptive laws (34)(35), can ensure that all signals of the closed-loop system are ultimately uniformly bounded. The system errors χ_i, e_i can be reduced arbitrarily by selecting appropriate control parameters.

P r o o f.   Choose the Lyapunov function

$$V = V_o + \sum_{i=1}^{n} V_i + \sum_{i=2}^{n} V_{i,h}, \tag{42}$$

where $V_i = \frac{1}{2} f_{zi}(\chi_i)\chi_i + \frac{1}{2\beta_i}\widetilde{\theta}_i^T\widetilde{\theta}_i + \frac{1}{2\gamma_i}\widetilde{\rho}_i^2$, $V_{i,h} = \frac{1}{2}h_i^2$. $h_i = z_i - \alpha_i$ is the first-order filter tracking error.

First, we consider the time interval $t \in \Phi(0, +\infty)$, and during this time period, $\breve{y} = 0, \vartheta = 0$. According to the Lyapunov function defined above, we have

$$V_1 = \frac{1}{2} f_{z1}(\chi_1)\chi_1 + \frac{1}{2\beta_1}\widetilde{\theta}_1^T\widetilde{\theta}_1 + \frac{1}{2\gamma_1}\widetilde{\rho}_1^2. \tag{43}$$

According to (43) and (26)–(29), the derivative of V_1 is

$$\dot{V}_1 = l_1(\chi_1)\left[\hat{\theta}_1^T S_1 - k_1^0\hat{x}_1 - \chi_2 + c_1\chi_1 - \alpha_2 + T_2\dot{z}_2 - \dot{y}_d\right] + \widetilde{\theta}_1^T\left[l_1(\chi_1)S_1 - \sigma_1\hat{\theta}_1\right]$$

$$+ \widetilde{\rho}_1\left[\tanh\left(\frac{l_1(\chi_1)}{\xi}\right)l_1(\chi_1) - \Lambda\left(\hat{\rho}_1 - \rho_1^0\right)\right]. \tag{44}$$

And then, according to Assumption 6 and Young's inequality, we have

$$-\sigma_i\hat{\theta}_i^T\widetilde{\theta}_i \le \frac{\sigma_i}{2}\theta_M^2 - \frac{\sigma_i}{2}\widetilde{\theta}_i^T\widetilde{\theta}_i \tag{45}$$

and

$$-\left(\hat{\rho}_i - \rho_i\right)\left(\hat{\rho}_i - \rho_i^0\right) \le -\frac{1}{2}\widetilde{\rho}_i^2 + \frac{1}{2}\left(\rho_i - \rho_i^0\right)^2. \tag{46}$$

As for a hyperbolic tangent function, when $\iota \in \mathbb{R}$, for any $\xi > 0$, the inequality $0 \le |\iota| - \iota\tanh\left(\frac{\iota}{\xi}\right) \le 0.2785\xi$ holds. According to (44)–(46) and the property of $\tanh(\cdot)$, (44) can be written as

$$\dot{V}_1 \le l_1(\chi_1)\left[\chi_2 - c_1\chi_1 - g_1l_1(\chi_1) - T_2\dot{z}_2\right] + 0.2785\xi\rho_1 + \frac{\sigma_1}{2}\theta_M^2 - \frac{\sigma_1}{2}\widetilde{\theta}_1^T\widetilde{\theta}_1$$

$$-\frac{\Lambda}{2}\widetilde{\rho}_1^2 + \frac{\Lambda}{2}\left(\rho_1 - \rho_1^0\right)^2. \tag{47}$$

Similarly, according to (31)–(41), (45) and (46), we obtain

$$\dot{V}_i \le l_i(\chi_i)\left[\chi_i - c_i\chi_i - g_il_i(\chi_i) - T_i\dot{z}_i - \frac{l_{i-1}(\chi_{i-1})}{N_i(\chi_i)}\right] + 0.2785\xi\rho_i + \frac{\sigma_i}{2}\theta_M^2 - \frac{\sigma_i}{2}\widetilde{\theta}_i^T\widetilde{\theta}_i$$

$$-\frac{\Lambda}{2}\widetilde{\rho}_i^2 + \frac{\Lambda}{2}\left(\rho_i - \rho_i^0\right)^2, \tag{48}$$

and

$$V_n \le l_n(\chi_n)\left[-c_n\chi_n - g_nl_n(\chi_n) - \frac{l_{n-1}(\chi_{n-1})}{N_n(\chi_n)}\right] + \frac{\sigma_n}{2}\theta_M^2 + 0.2785\xi\rho_n - \frac{\sigma_n}{2}\widetilde{\theta}_n^T\widetilde{\theta}_n - \frac{\Lambda}{2}\widetilde{\rho}_n^2$$

$$+ \frac{\Lambda}{2}\left(\rho_n - \rho_n^0\right)^2. \tag{49}$$

From (36) and (42), the derivative of tracking error of first-order filter is

$$\dot{h}_i = -\frac{h_i}{T_i} z_i - \dot{\alpha}_i. \tag{50}$$

According to (27), (33) and Assumption 1–Assumption 7, there exists a differentiable continuous function $\varphi(\cdot)$ satisfying

$$|\dot{\alpha}_i| \leq \varphi\left(\chi_i, h_i, \widetilde{\theta}_i, \widetilde{\rho}_i, T_i, g_i, c_i, k_i^{\vartheta}, y_d, \dot{y}_d, \ddot{y}_d\right). \tag{51}$$

For $C_0 > 0$ and $\varpi > 0$, the set $\Omega_1 = \left\{(y_d, \dot{y}_d, \ddot{y}_d)\,|\,y_d^2 + \dot{y}_d^2 + \ddot{y}_d^2 \leq C_0\right\} \in \mathbb{R}^3$ in Assumption 1 and $\Omega_2 = \{(\chi_i, \theta_i, h_i, \rho_i, e_i)\,|\,V \leq \varpi\} \in \mathbb{R}^{\sum_{p=1}^{i} p+4i-1}$ are compact sets. And then, the function $\varphi(\cdot)$ has a maximum value M over the compact set $\Omega_1 \times \Omega_2 \in \mathbb{R}^{\sum_{p=1}^{i} p+4i+2}$. Thus, one has

$$\dot{V}_{i,h} \leq -\left(\frac{1}{T_i} - \frac{1}{2}\right) h_i^2 + \frac{M^2}{2}. \tag{52}$$

According to Property 1–Property 3 of the nonlinear gain function in Section II and the Young's inequality, we have

$$l_i\left(\chi_i\right) h_i \leq \zeta_i l_i^2\left(\chi_i\right) + \frac{1}{4\zeta_i} h_i^2 \tag{53}$$

and

$$-l_i\left(\chi_i\right) c_i \chi_i \leq -\frac{1}{2} f_{z_i}\left(\chi_i\right) c_i \chi_i. \tag{54}$$

From (42), and (44)–(54), the derivative of V yields

$$\dot{V} \leq e^T \left[A^T P^0 + P^0 A + 2P^0 P^0 + 2\sum_{i=1}^{n} m_i^2 + \hat{x}_1^2 P^0 K^0 K^{0T} P^0 \right] e - \sum_{i=1}^{n} \frac{1}{2} f_{z_i}\left(\chi_i\right) c_i \chi_i$$
$$- \sum_{i=1}^{n} \frac{\sigma_i}{2} \widetilde{\theta}_i^T \widetilde{\theta}_i - \sum_{i=1}^{n} \frac{\Lambda}{2} \widetilde{\rho}_i^2 - \sum_{i=2}^{n} \left(\frac{1}{T_i} - \frac{1}{2} - \frac{1}{4\zeta_i}\right) h_i^2 + \sum_{i=1}^{n} 0.2785 \xi \rho_i + \sum_{i=1}^{n} \frac{\sigma_i}{2} \theta_M^2$$
$$+ \sum_{i=1}^{n} \frac{\Lambda}{2}\left(\rho_i - \rho_i^0\right)^2 + \sum_{i=2}^{n} \frac{M^2}{2} + \|\delta_M\|^2 + M_o. \tag{55}$$

Then, we consider of time interval $t \in \Psi(0, +\infty)$, and during this time period, $\breve{y} = x_1, \vartheta = 1$. Similarly, the derivative of V yields

$$\dot{V} \leq e^T \left[\left(A - K^1 C_0\right)^T P^1 + P^1 \left(A - K^1 C_0\right) + 2P^0 P^0 + 2\sum_{i=1}^{n} m_i^2 \right] e - \sum_{i=1}^{n} \frac{1}{2} f_{z_i}\left(\chi_i\right) c_i \chi_i$$
$$- \sum_{i=1}^{n} \frac{\sigma_i}{2} \widetilde{\theta}_i^T \widetilde{\theta}_i - \sum_{i=1}^{n} \frac{\Lambda}{2} \widetilde{\rho}_i^2 - \sum_{i=2}^{n} \left(\frac{1}{T_i} - \frac{1}{2} - \frac{1}{4\zeta_i}\right) h_i^2 + \sum_{i=1}^{n} 0.2785 \xi \rho_i + \sum_{i=1}^{n} \frac{\sigma_i}{2} \theta_M^2$$
$$+ \sum_{i=1}^{n} \frac{\Lambda}{2}\left(\rho_i - \rho_i^0\right)^2 + \sum_{i=2}^{n} \frac{M^2}{2} + \|\delta_M\|^2 + M_o. \tag{56}$$

Further, we prove the overall stability of the closed-loop system by the ADT method in [46, 47].

According to the above analysis, the results (55)(56) can be expressed as

$$\dot{V} \leq \pi(t)V + C, \tag{57}$$

where $\pi(t) = \upsilon$ when $t \in \Phi(0, +\infty)$ and $\pi(t) = -\nu$ when $t \in \Psi(0, +\infty)$; $C = \sum_{i=1}^{n} 0.2785\xi\rho_i + \sum_{i=1}^{n} \frac{\sigma_i}{2}\theta_M^2 + \sum_{i=1}^{n} \frac{\Lambda}{2}\left(\rho_i - \rho_i^0\right)^2 + \sum_{i=2}^{n} \frac{M^2}{2} + \|\delta_M\|^2 + M_o$.

As mentioned in Section 2, the time variable t_k represents the time when the kth DoS attack becomes active. For $t \in [t_k, t_{k+1})$, we denote $\pi(t) = \pi_k$, and the Lyapunov function V yields

$$
\begin{aligned}
V(t) &\leq \exp(\pi_k\,(t - t_k))V\,(t_k) + C\int_{t_k}^{t} \exp(\pi_k(t - \tau))\,\mathrm{d}\tau \\
&\leq \mu\exp(\pi_k\,(t - t_k))V\,(t_k^-) + C\int_{t_k}^{t} \exp(\pi_k(t - \tau))\,\mathrm{d}\tau.
\end{aligned}
\tag{58}
$$

Using the iterative method in [47], (58) can be rewrite as

$$
\begin{aligned}
V(t) \leq& \mu^{n(0,t)}\exp(-(\nu|\Psi(0,t)| - \upsilon|\Phi(0,t)|))V(0) \\
&+ C\int_{0}^{t} \mu^{n(\tau,t)}\exp(-(\nu|\Psi(\tau,t)| - \upsilon|\Phi(\tau,t)|))\,\mathrm{d}\tau \\
\leq& \exp(-(\nu|\Psi(0,t)| - \upsilon|\Phi(0,t)| - n(0,t)\ln\mu))V(0) \\
&+ C\int_{0}^{t} \exp(-(\nu|\Psi(\tau,t)| - \upsilon|\Phi(\tau,t)| - n(\tau,t)\ln\mu))\,\mathrm{d}\tau.
\end{aligned}
\tag{59}
$$

According to Assumption 5, during the period $[\tau, t]$, we have $|\Phi(\tau,t)| \leq \omega + \frac{t-\tau}{\varrho}$ and $|\Psi(\tau,t)| \geq \left(1 - \frac{1}{\varrho}\right)(t - \tau) - \omega$. By virtue of the ADT method with Assumption 4–Assumption 5, $[(\upsilon - \pi^*)/(\nu + \upsilon)] > \frac{1}{\varrho}$ and $\tau_D > \frac{\ln\mu}{\pi^*}$, there exists a constant $\varsigma > 0$ satisfying $\nu|\Psi(\tau,t)| - \upsilon|\Phi(\tau,t)| > \pi^*(t-\tau) - \omega(\nu+\upsilon) > (n(\tau,t)-\kappa)\ln\mu + \varsigma(t-\tau) - \omega(\nu+\upsilon)$. Hence,

$$V(t) \leq \mu^{\kappa}\exp[\omega(\nu + \upsilon)]\left[\exp(-\varsigma t)V(0) + \frac{C}{\varsigma}\right]. \tag{60}$$

From (59) and (60), with a sufficiently large constant ν, there exists a constant ℓ, the inequality $\mu^{\kappa}\exp[\omega(\nu + \upsilon)](C/\varsigma) \leq \ell^2$ holds. It comes the results that $\lim_{t\to\infty}\|e\| \leq \frac{2\ell}{\sqrt{\lambda_{\min}(P)}}$, $\lim_{t\to\infty}|\chi_1| \leq 2\ell$ and $\lim_{t\to\infty}|\epsilon| = \lim_{t\to\infty}|\chi_1 + e_1| \leq 2\ell + \frac{2\ell}{\sqrt{\lambda_{\min}(P)}}$. According to (42), $\widetilde{\theta}_i$, $\widetilde{\rho}_i$ and h_i are ultimately bounded. From (31)(33) and (36), $\hat{x}_i$, α_i and z_i are also bounded. In addition, due to the bound of $\widetilde{\rho}_i$ and ρ_i, it follows that $\hat{\rho}_i$ is bounded. Therefore, all signals in the closed-loop system are ultimately bounded.

$\square$

Remark 4.2. Similarly to [42, 46], in this paper, the ADT method is applied in stability analysis. It should be pointed out that there exist two situations of the system, suffering from and free from the attack in this paper. The individual subsystem is different from a normal switching system, and the traditional ADT methods might not be applied directly. To address the secure control issue, we improve the traditional average dwell-time method and pose additional conditions from Theorem 4.1, such as unstable duration concept, onto the paralyzed system.

Remark 4.3. The increasement of frequency and duration of DoS attack has an impact on control performance. On one hand, from Theorem 4.1 in this paper, to obtain the stability of the whole closed-loop system, the following conditions are posed with $[(v - \pi^*)/(\nu + \upsilon)] > \frac{1}{\varrho}$ and $\tau_D > \frac{\ln \mu}{\pi^*}$. For a given attack number, the duration of DoS in the time interval $[\tau, t]$ is scaled up, that is $|\Phi(\tau, t)|$ is extended. Accordingly, ϱ decreases, and according to those inequality conditions and assumptions of attack properties, the values of τ_D will augment. It follows the result that κ is going to increase. Thus, we obtain that the size of the tracking error ϵ will be larger and system control performance will be degraded. On the other hand, once the value of τ_k is too large, parameter ϱ does not satisfy the additional conditions, and it means that the parameter π^* does not exist and the system stable results is not available. This may lead to instability of the closed-loop system.

5. SIMULATION RESULTS

In order to verify the effectiveness of the proposed control strategy, the simulation results on a flexible-joint manipulator and a numerical example are presented.

5.1. Flexible-joint manipulator

The model of a flexible-joint manipulator is

$$A_0 \ddot{r} + B_0 \dot{r} + mgl \cos r = \alpha + d_{is}, \tag{61}$$

where $A_0 = 4ml^2/3$ is the moment of inertia, B_0 is coefficient of viscous friction, m is the mass of the manipulator, l is the distance between the center of mass and the rotation center of the connecting rod, r is the output angle, α is the moment of the manipulator, and d_{is} represents external disturbances. Denote $x_1 = r$, $x_2 = \dot{r}$ and $u = \alpha$, and the dynamic equation (61) can be further written as

$$\begin{cases} \dot{x}_1 = x_2, \\ \dot{x}_2 = -\dfrac{3}{2ml^2} x_2 - \dfrac{3g}{4l} \cos x_1 + \dfrac{3}{4ml^2} u + \dfrac{3d_{is}}{4ml^2}, \\ y = x_1, \end{cases} \tag{62}$$

where $m = 1$kg, $l = 0.25$m, $g = 9.8$N/kg, $d_{is} = x_2 \sin x_1$, and the initial values of angular position and angular velocity are $[x_1(0), x_2(0)]^T = [0.1, 0.5]^T$. The desired position is $y_d = \sin(t)$, and the parameter of the DoS are $\tau_D = 3.3$ and $\varrho = 5.1$. The parameters are $\lambda = 1$, $g_1 = 60$, $g_2 = 60$, $c_1 = 30$, $c_2 = 30$, $\beta_1 = 0.5$, $\beta_2 = 3$, $\sigma_1 = 10$, $\sigma_2 = 10$,

$\gamma_1 = 100$, $\gamma_2 = 100$, $\Lambda = 10$, $\rho_1^0 = 1$, $\rho_2^0 = 300$ and $\xi = 1, T_2 = 1$. The number of hidden layer nodes in RBF NNs is 11, and the input vector of the first NNs and the second one are $Z_1 = \begin{bmatrix} \hat{x}_1, \hat{x}_{2,f} \end{bmatrix}^T$ a nd $Z_2 = \begin{bmatrix} \hat{x}_1, \hat{x}_2, u_f \end{bmatrix}^T$, respectively. We choose $b_j = \begin{bmatrix} b_{j,1}, b_{j,2} \end{bmatrix}^T$ and $b_j = \begin{bmatrix} b_{j,1}, b_{j,2}, b_{j,3} \end{bmatrix}^T$, for the first and second NNs, where $b_{j,1}$ and $b_{j,2}$ evenly space in $\begin{bmatrix} -1.5, 1.5 \end{bmatrix}$ and $\begin{bmatrix} -2.5, 2.5 \end{bmatrix}$, respectively, $b_{j,3}$ is between $[-5, 5]$, $\eta_1 = 0.1$, $\eta_2 = 20$ and the initial weights are $\hat{\theta}_1(0) = 0.1I_{11}$ and $\hat{\theta}_2(0) = 0.5I_{11}$. Choose $\upsilon = 10$, $\nu = 5$, and $\mu = 540$, $K^0 = \begin{bmatrix} 101.7854, 203.2549 \end{bmatrix}^T$, $K^1 = \begin{bmatrix} 1.1547, 1.0126 \end{bmatrix}^T$. The simulation results are shown in Figure 3 – Figure 6 with DoS attack interval shown in the first subfigure of Figure 3. The second subfigure of Figure 3 and Figure 4 are tracking trajectories and control input signal in the presence of the DoS attack, respectively. Figure 5 shows the approximation behavior of the unknown function F_2, and the norm of the estimation weight. It is seen, from Figure 6, that internal states, x_1 and x_2, of the system are reconstructed by the observer.
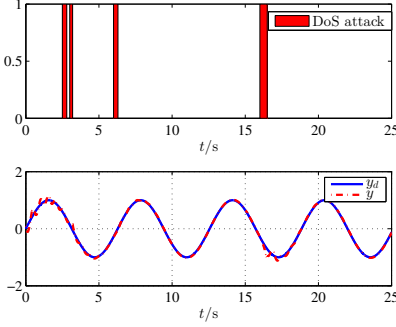
Fig. 3: DoS attack and tracking performance (Example A)
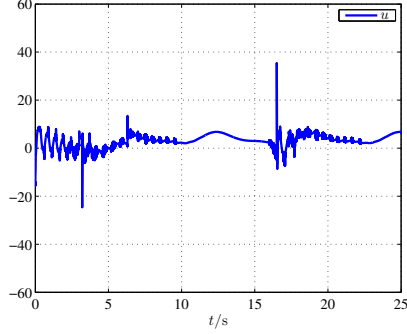

Fig. 4: Control input signal (Example A)

To illustrate the importance of the observer with switching gain in the secure control, its performance in this paper is compared with that of the traditional NNs observer in [4]. It can be seen that, from Figure 7, the traditional NN observer cannot estimate the system state accurately when DoS attack is active, and it cause ineffectual control. In contrast, the NNs observer with switching gain in this paper is able to reconstruct unknown states in the presence of the DoS attack. This is due to the fact that the observer we designed is on the basis switching system technology [44, 45, 47], and it guarantees the stability of the system either the attacked or non-attacked period.

To show the advantage of the recursive sliding-mode, the strategy proposed in this paper is compared with the method in [38]. Three cases of the control parameters are listed in Table 1. From Figure 8, it indicates that, if the parameters T_2 and β_i are chosen appropriately, both the method in this paper and the one in [38] are robust to the uncertainties. Nevertheless, if T_2 and β_i are too large, the control signal in [38] oscillates violently while the control signals of the method proposed in this paper is still smooth and stable. The phenomenon shows that the proposed strategy can release the sensitiveness to perturbation in both the filter time constant and adaptive parameters.
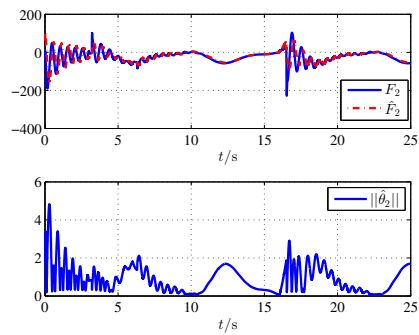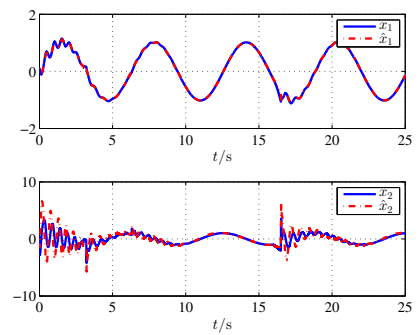
Fig. 5: NNs performance (Example A)

Fig. 6: Observer performance (Example A)

Case	Adaptive parameters	Filter parameter
1	$\beta_1 = \beta_2 = 5$	$T_2 = 0.1$
2	$\beta_1 = \beta_2 = 5$	$T_2 = 0.8$
3	$\beta_1 = \beta_2 = 500$	$T_2 = 0.1$

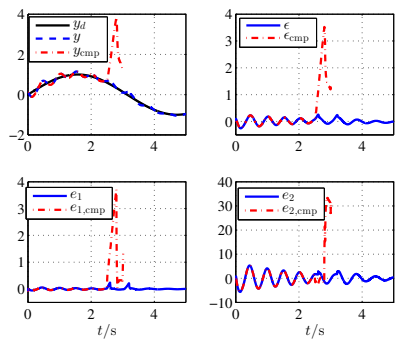**Tab. 1:** Different adaptive parameters and filter time parameters

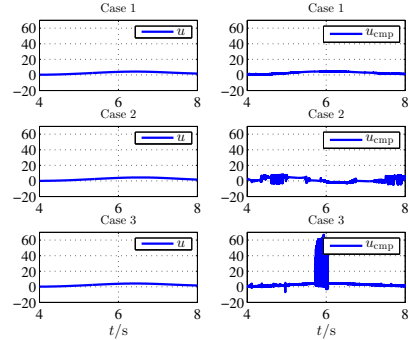**Fig. 7:** Comparison of the observer performance. (Example A)

Fig. 8: Control input signal comparison in Table 1 (Example A)

5.2. Numerical example

We consider a non-affine pure-feedback nonlinear system

$$\begin{cases} \dot{x}_1 = \cos\left(x_1 + x_2\right) + 2x_2, \\ \dot{x}_2 = \sin\left(2x_1\right) + 2x_3 + \cos\left(2x_2 + x_3\right), \\ \dot{x}_3 = \cos\left(x_1 x_2 x_3\right) + u + 0.1\cos u. \end{cases} \tag{63}$$

The parameters of the DoS attack are $\tau_D = 2.1$ and $\varrho = 6.3$. The secure strategy is designed as (39) with $g_1 = 4$, $g_2 = 4$, $g_3 = 4$, $c_1 = 5$, $c_2 = 5$, $c_3 = 5$, $\beta_1 = 0.1$, $\beta_2 = 10$, $\beta_3 = 10$, $\sigma_1 = 10$, $\sigma_2 = 5$, $\sigma_3 = 5$, $\gamma_1 = 0.1$, $\gamma_2 = 0.5$, $\gamma_3 = 0.8$, $\Lambda = 8$, $\rho_1^0 = 10$, $\rho_2^0 = 5$, $\rho_3^0 = 1$, $\xi = 0.01$, $\lambda = 1$, and time constants of the two filters $T_2 = T_3 = 1$. The number of hidden layer nodes in RBF NNs is 9, and the input vectors of the three NNs are $Z_1 = \left[\hat{x}_1, \hat{x}_{2,f}\right]^T$, $Z_2 = \left[\hat{x}_1, \hat{x}_2, \hat{x}_{3,f}\right]^T$ and $Z_3 = \left[\hat{x}_1, \hat{x}_2, \hat{x}_3, u_f\right]^T$, respectively. We choose $b_j = \left[b_{j,1}, b_{j,2}\right]^T$ for the first NNs, $b_j = \left[b_{j,1}, b_{j,2}, b_{j,3}\right]^T$ for the second NNs, and $b_j = \left[b_{j,1}, b_{j,2}, b_{j,3}, b_{j,4}\right]^T$ for the third NNs, where $b_{j,1}$ and $b_{j,2}$ is evenly distributed between $\left[-2, 2\right]$, $b_{j,3}$ is between $\left[-3, 3\right]$, $b_{j,4}$ is between $\left[-10, 10\right]$. We select the Gaussian width $\eta_1 = 10, \eta_2 = 20, \eta_3 = 1$ and the initial weight of NNs $\hat{\theta}_1(0) = \hat{\theta}_2(0) = \hat{\theta}_3(0) = 0.1 I_9$. Choose $\upsilon = 12$, $\nu = 4$, and $\mu = 580$, $K^0 = \left[101.4795, 100.8563, 100.0023\right]^T$, $K^1 = \left[50.0213, 52.0104, 50.1032\right]^T$. The desired trajecory is $y_d = \sin(t)$. Figure 9 shows the tracking performance inspite of the DoS attack. Figure 10 and Figure 11 depict the control input signal and the observer performance, respectively.
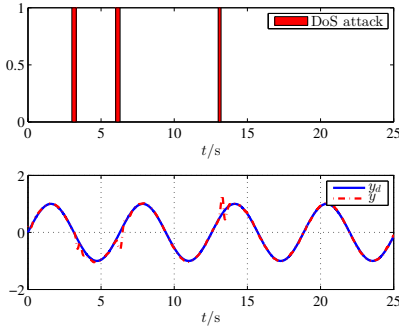

Fig. 9: DoS attack and tracking performance (Example B)
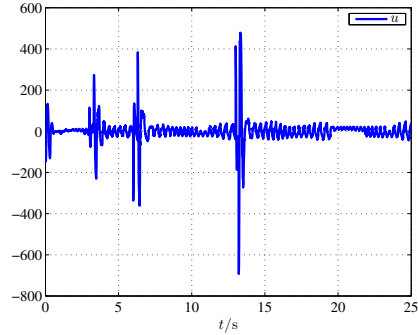

Fig. 10: Control input signal (Example B)

To illustrate the advantage of the secure control strategy in this paper, we compare the control performance under the adaptive method in [20] suffered from the same attack. It can be seen from Figure 12 that the secure control strategy proposed in this paper perform better than the adaptive control method in [20] does. The system crashes directly under control method [20] and cannot work against the Dos attack. This is because the switching type NN observer in the strategy is introduced here to reconstruct internal state via discontinuous output information.
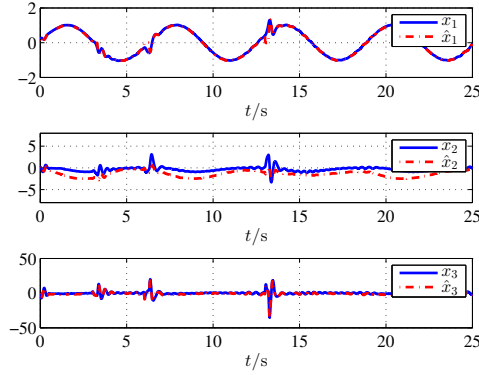
Fig. 11: Observer performance (Example B)

Case	DoS attack parameters
1	$\varrho = 5.9,\ \tau_D = 2.8$
2	$\varrho = 4.9,\ \tau_D = 3.5$
3	$\varrho = 4.3,\ \tau_D = 4.0$

Tab. 2: Different attack parameters in Example B

To further verify the impact, the frequency and duration from DoS attack, on system performance, three cases of DoS attack parameters are listed in Table 2. The comparison results of the control performance are shown in Figure 13. It can be seen that, as the duration of DoS attack increases, the tracking error also increases and the control performance is degraded. Once the parameter of the attack does not satisfy the inequality condition $[(v - \pi^*)/(\nu + \upsilon)] > \frac{1}{\varrho}$ and $\tau_D > \frac{\ln \mu}{\pi^*}$, it implies that the parameter π^* is not available. The red line in Figure 8 means that the system, suffered from such attack with the parameters in Case 3, is unstable. This is consistent with the analysis results in Remark 4.3.

6. CONCLUSION

In this paper, an adaptive secure control strategy with nonlinear gain and recursive sliding-mode has been designed for a networked non-affine nonlinear system under DoS attacks. The NN-based observer with switching gains has been developed for unmeasurable states, and the recursive sliding-mode has been for the problem of being sensitive to the perturbation of control parameters in traditional NNs DSC method. Also, the nonlinear gain function has been introduced for a compromise between the control accuracy and dynamic performance. Based on Lyapunov theory, combining switching type technology with ADT method, it has proved that the designed secure control strategy guarantees the ultimate boundedness of all signals in the closed-loop system.
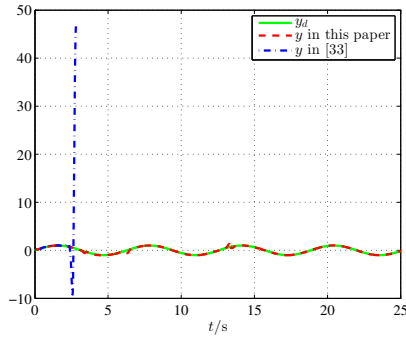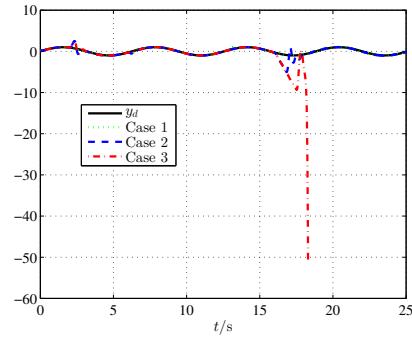
Fig. 12: Control performance comparison (Example B)

Fig. 13: Control performance comparison in Tab. 2 (Example B)

ACKNOWLEDGEMENT

REFERENCES

[1] L. An and G. H. Yang: Decentralized adaptive fuzzy secure control for nonlinear uncertain interconnected systems against intermittent dos attacks. IEEE Trans. Cybernet. *49* (2019), 3, 827–838. DOI:10.1109/tcyb.2017.2787740

[2] A. Boubakir, S. Labiod, and F. Boudjema: Linear adaptive control of a class of SISO nonaffine nonlinear systems. Int. J. Systems Sci. *45* (2014), 12, 2490–2498. DOI:10.1080/00207721.2013.772259

[3] W. Chen, D. Ding, X. Ge, Q. L. Han, and G. Wei: H_∞ containment control of multi-agent systems under event-triggered communication scheduling: The finite-horizon case. IEEE Trans. Cybernet. (2018) 1–11. DOI:10.1109/tcyb.2018.2885567

[4] B. Chen, H. Zhang, and C. Lin: Observer-based adaptive neural network control for nonlinear systems in nonstrict-feedback form. IEEE Trans. Neural Networks Learning Systems *27* (2017), 1, 89–98. DOI:10.1109/tnnls.2015.2412121

[5] P. Gahinet, A. Nemirovskii, and A. J. Laub: The LMI control toolbox. In: Proc. 33rd IEEE Conference on Decision and Control, IEEE *3* (1994), pp. 2038–2041. DOI:10.1109/cdc.1994.411440

[6] X. Ge and Q. L. Han: Consensus of multiagent systems subject to partially accessible and overlapping Markovian network topologies. IEEE Trans. Cybernet. *47* (2017), 8, 1807–1819. DOI:10.1109/tcyb.2016.2570860

[7] L. Ding, Q. L. Han, and X. Ge: An overview of recent advances in event-triggered consensus of multiagent systems. IEEE Trans. Cybernet. *48* (2018), 4, 1110–1123. DOI:10.1109/tcyb.2017.2771560

[8] D. Ding, Z. Wang, Q. L. Han, and G. Wei: Neural-network-based output-feedback control under Round–Robin scheduling protocols. IEEE Trans. Cybernet. *49* (2019), 6, 2372–2384. DOI:10.1109/tcyb.2018.2827037

[9] V. S. Dolk, P. Tesi, and C. D. Persis: Event-triggered control systems under denial-of-service attacks. IEEE Trans. Control Network Syst. *4* (2016), 1, 93–105. DOI:10.1109/tcns.2016.2613445

[10] X. Ge, Q. L. Han, and Z. Wang: A dynamic event-triggered transmission scheme for distributed set-membership estimation over wireless sensor networks. IEEE Trans. Cybernetics *49* (2019), 1, 171–183. DOI:10.1109/tcyb.2017.2769722

[11] X. Ge, Q. L. Han, and X. M. Zhang: Achieving cluster formation of multi-agent systems under aperiodic sampling and communication delays. IEEE Trans. Industr. Electron. *65* (2018), 4, 3417–3426. DOI:10.1109/tie.2017.2752148

[12] S. Hu, D. Yue, and X. Xie: Resilient event-triggered controller synthesis of networked control systems under periodic dos jamming attacks. IEEE Trans. Cybernet. *49* (2018), 12, 4271–4281. DOI:10.1109/tcyb.2018.2861834

[13] D. Ding, Q. L. Han, Z. Wang, and X. Ge: A survey on model-based distributed control and filtering for industrial cyber-physical systems. IEEE Trans. Industr. Inform. *15* (2019), 5, 2483–2499. DOI:10.1109/tii.2019.2905295

[14] A. Farraj, E. Hammad, and D. Kundur: A cyber-physical control framework for transient stability in smart grids. IEEE Trans. Smart Grid *9* (2018), 2, 1205–1215. DOI:10.1109/tsg.2016.2581588

[15] X. Ge, Q. L. Han, and Z. Wang: A threshold-parameter-dependent approach to designing distributed event-triggered H_∞ consensus filters over sensor networks. IEEE Trans. Cybernet. *9* (2019), 4, 1148–1159. DOI:10.1109/tcyb.2017.2789296

[16] A. Kulkarni and S. Purwar: Adaptive nonlinear gain based composite nonlinear feedback controller with input saturation. IMA J. Math. Control Inform. *3* (2018), 35, 757–771. DOI:10.1093/imamci/dnw075

[17] Y. Li and S. Tong: Prescribed performance adaptive fuzzy output-feedback dynamic surface control for nonlinear large-scale systems with time delays. Inform. Sci. *29* (2015), 125–142. DOI:10.1016/j.ins.2014.08.060

[18] Y. Li, S. Tong, and T. Li: Adaptive fuzzy output feedback dynamic surface control of interconnected nonlinear pure-feedback systems. IEEE Trans. Cybernet. *45* (2014), 1, 138–149. DOI:10.1109/tcyb.2014.2333738

[19] X. Liu and X. Sun: Non-fragile recursive sliding mode dynamic surface control with adaptive neural network. Control Theory Appl. *30* (2013), 10, 1323–1328.

[20] X. Liu and X. Sun: Recursive sliding-mode dynamic surface adaptive NN control with nonlinear gains. Acta Automat. Sinica *40* (2014), 10, 2193–2202.

[21] A. Y. Lu and G. H. Yang: Input-to-state stabilizing control for cyber-physical systems with multiple transmission channels under denial of service. IEEE Trans. Automat. Control *63* (2018), 6, 1813–1820. DOI:10.1109/tac.2017.2751999

[22] C. Lv, Y. Liu, and X. Hu: Simultaneous observation of hybrid states for cyber-physical systems: A case study of electric vehicle powertrain. IEEE Trans. Cybernet. *48* (2018), 8, 2357–2367. DOI:10.1109/tcyb.2017.2738003

[23] B. Niu, H. Li, and T. Qin: Adaptive NN dynamic surface controller design for nonlinear pure-feedback switched systems with time-delays and quantized input. IEEE Trans. Systems Man Cybernet.: Systems. *48* (2017), 10, 1676–1688. DOI:10.1109/tsmc.2017.2696710

[24] J. Otto, B. Vogel-Heuser, and O. Niggemann: Automatic parameter estimation for reusable software components of modular and reconfigurable cyber-physical production systems in the domain of discrete manufacturing. IEEE Trans. Industr. Inform. *14* (2018), 1, 275–282. DOI:10.1109/tii.2017.2718729

[25] C. D. Persis and P. Tesi: Input-to-state stabilizing control under denial-of-service. IEEE Trans. Automat. Control. *60* (2015), 11, 2930–2944. DOI:10.1109/tac.2015.2416924

[26] J. Qin, M. Li, and L. Shi: Optimal denial-of-service attack scheduling with energy constraint over packet-dropping networks. IEEE Trans. Automat. Control *63* (2018), 6, 1648–1663. DOI:10.1109/tac.2017.2756259

[27] Z. Shen: Recursive sliding mode dynamic surface output feedback control for ship trajectory tracking based on neural network observer. Control Theory Appl. *35* (2018), 8, 1092–1100.

[28] Z. Shen and X. Zhang: Recursive sliding-mode dynamic surface adaptive control for ship trajectory tracking with nonlinear gains. Acta Automat. Sinica *44* (2018), 10, 1833–1841.

[29] X. Shi, C. C. Lim, and P. Shi: Adaptive neural dynamic surface control for nonstrict-feedback systems with output dead zone. IEEE Trans. Neural Networks Learning Systems *29* (2018), 11, 5200–5213. DOI:10.1109/tnnls.2018.2793968

[30] H. Sun, C. Peng, and W. Zhang: Security-based resilient event-triggered control of networked control systems under denial of service attacks. J. Franklin Inst. *356* (2018), 17, 10277–10295. DOI:10.1016/j.jfranklin.2018.04.001

[31] Y. C. Sun and G. H. Yang: Periodic event-triggered resilient control for cyber-physical systems under denial-of-service attacks. J. Franklin Inst. *355* (2018), 13, 5613–5631. DOI:10.1016/j.jfranklin.2018.06.009

[32] Y. C. Sun and G. H. Yang: Event-triggered resilient control for cyber-physical systems under asynchronous DoS attacks. Inform. Sci. *465* (2018), 340–352. DOI:10.1016/j.ins.2018.07.030

[33] D. Swaroop, J. K. Hedrick, and P. P. Yip: Dynamic surface control for a class of nonlinear systems. IEEE Trans. Automat. Control *45* (2000), 10, 1893–1899. DOI:10.1109/tac.2000.880994

[34] E. Tian, Z. Wang, L. Zou, and D. Yue: Chance-constrained H_∞ control for a class of time-varying systems with stochastic nonlinearities: The finite-horizon case. Automatica *107* (2019), 296–305. DOI:10.1016/j.automatica.2019.05.039

[35] E. Tian, Z. Wang, L. Zou, and D. Yue: Probabilistic-constrained filtering for a class of nonlinear systems with improved static event-triggered communication. Internat. J. Robust Nonlinear Control *29* (2019), 5, 1484–1498. DOI:10.1002/rnc.4447

[36] S. Tong, Y. Li, and X. Jing: Adaptive fuzzy decentralized dynamics surface control for nonlinear large-scale systems based on high-gain observer. Inform. Sci. *235* (2013), 287–307. DOI:10.1016/j.ins.2013.02.033

[37] Y. Wang, Y. Gao, and H. R. Karimi: Sliding mode control of fuzzy singularly perturbed systems with application to electric circuit. IEEE Trans. Systems Mand Cybernet.: Systems *48* (2017), 10, 1667–1675. DOI:10.1109/tsmc.2017.2720968

[38] D. Wang and J. Huang: Neural network-based adaptive dynamic surface control for a class of uncertain nonlinear systems in strict-feedback form. IEEE Trans. Neural Networks *16* (2005), 1, 195–202. DOI:10.1109/tnn.2004.839354

[39] L. Wu, Y. Gao, and J. Liu: Event-triggered sliding mode control of stochastic systems via output feedback. Automatica *82* (2017), 79–92. DOI:10.1016/j.automatica.2017.04.032

[40] L. Xu, Q. Guo, and T. Yang: Robust routing optimization for smart grids considering cyber-physical interdependence. IEEE Trans. Smart Grid *10* (2018), 5, 5620–5629. DOI:10.1109/tsg.2018.2888629

[41] X. Ye: Global adaptive control of nonlinearly parametrized systems. IEEE Trans. Automat. Control *48* (2003), 1, 169–173. DOI:10.1109/tac.2002.804464

[42] J. Yang, Y. Chen, and L. Cui: Multiple-mode adaptive state estimator for nonlinear switched systems. Int. Control Automat. Syst. *15* (2017), 4, 1485–1493. DOI:10.1007/s12555-016-0331-0

[43] J. Yu, Y. Ma, and H. Yu: Adaptive fuzzy dynamic surface control for induction motors with iron losses in electric vehicle drive systems via backstepping. Inform. Sci. *376* (2017), 172–189. DOI:10.1016/j.ins.2016.10.018

[44] Q. Yu and B. Wu: Robust stability analysis of uncertain switched linear systems with unstable subsystems. Int. J. Systems Sci. *46* (2015), 7, 1278–1287. DOI:10.1080/00207721.2013.816089

[45] D. Zhai, L. An, and J. Dong: Switched adaptive fuzzy tracking control for a class of switched nonlinear systems under arbitrary switching. IEEE Trans. Fuzzy Syst. *26* (2018), 2, 585–597. DOI:10.1109/tfuzz.2017.2686378

[46] G. Zhai, B. Hu, and K. Yasuda: Stability analysis of switched systems with stable and unstable subsystems: an average dwell time approach. Int. J. Systems Sci. *32* (2001), 8, 1055–1061. DOI:10.1080/00207720116692

[47] D. Zhai, C. Xi, and L. An: Prescribed performance switched adaptive dynamic surface control of switched nonlinear systems with average dwell time. IEEE Trans. Systems Man Cybernet.: Systems *47* (2017), 7, 1257–1269. DOI:10.1109/tsmc.2016.2571338

[48] H. Zhang, P. Cheng, and L. Shi: Optimal denial-of-service attack scheduling with energy constraint. IEEE Trans. Automat. Control *60* (2015), 11, 3023–3028. DOI:10.1109/tac.2015.2409905

[49] T. P. Zhang and S. S. Ge: Adaptive dynamic surface control of nonlinear systems with unknown dead zone in pure feedback form. Automatica *44* (2008), 7, 1895–1903. DOI:10.1016/j.automatica.2007.11.025

[50] X. M. Zhang, Q. L. Han, and X. Ge: Networked control systems: A survey of trends and techniques. IEEE/CAA J. Automat. Sinica (2019), 1–17. DOI:10.1109/jas.2019.1911651

[51] T. Zhang, M. Xia, and Y. Yi: Adaptive neural dynamic surface control of pure-feedback nonlinear systems with full state constraints and dynamic uncertainties. IEEE Trans. Systems Man Cybernet.: Systems. *47* (2017), 8, 2378–2387. DOI:10.1109/tsmc.2017.2675540

[52] Z. Zuo, Q. L. Han, and B. Ning: An overview of recent advances in fixed-time cooperative control of multi-agent systems. IEEE Trans. Industr. Informat. *14* (2018), 6, 2322–2334. DOI:10.1109/tii.2018.2817248

[53] A. M. Zou, Z. G. Hou, and M. Tan: Adaptive control of a class of nonlinear pure-feedback systems using fuzzy backstepping approach. IEEE Trans. Fuzzy Syst. *16* (2008), 4, 886–897. DOI:10.1109/tfuzz.2008.917301

Yang Yang, Corresponding author. College of Automation and the College of Artificial Intelligence, Nanjing University of Posts and Telecommunications, Nanjing 210023. P. R. China.
   e-mail: yyang@njupt.edu.cn

Qing Meng, College of Automation and the College of Artificial Intelligence, Nanjing University of Posts and Telecommunications, Nanjing 210023. P. R. China.

Dong Yue, College of Automation and the College of Artificial Intelligence, Institute of Advanced Technology, Jiangsu Engineering Laboratory of Big Data Analysis and Control for Active Distribution Network, Nanjing University of Posts and Telecommunications, Nanjing 210023. P. R. China.
   e-mail: medongy@vip.163.com

Tengfei Zhang, College of Automation and the College of Artificial Intelligence, Jiangsu Engineering Laboratory of Big Data Analysis and Control for Active Distribution Network, Nanjing University of Posts and Telecommunications, Nanjing 210023. P. R. China.

Bo Zhao, College of Automation and the College of Artificial Intelligence, Nanjing University of Posts and Telecommunications, Nanjing 210023. P. R. China.

Xiaolei Hou, NARI Group Corporation (State Grid Electric Power Research Institute), Nanjing 211000. P. R. China.